1-1-1990

The neutronic design of a university scale reactor for cold neutron research

Erik Boyd Iverson
Iowa State University

The neutronic design of a university scale reactor for cold neutron research

by

Erik Boyd Iverson

A Thesis Submitted to the
Graduate Faculty in Partial Fulfillment of the
Requirements for the Degree of
MASTER OF SCIENCE

Department: Mechanical Engineering
Major: Nuclear Engineering

Iowa State University
Ames, Iowa

1990

TABLE OF CONTENTS

I. INTRODUCTION

Research involving cold neutrons has increased at a steady rate in recent years. The utility and efficacy of low-energy neutrons in the study of various materials have made such neutrons a popular, valuable research tool. Unfortunately, there are few facilities providing cold neutron sources (at least in the United States). Furthermore, such facilities are very large and expensive, and "user-programs" to make them more available to the general research community are crowded.

Our goal is to design a type of cold neutron source that will be available to the entire research community. The source will be a small reactor, on the order of 10-100 kW, as opposed to currently available reactor sources, which often have a power in the range of 10-100 MW. This decrease in power is possible because, in the design presented here, all neutrons are dedicated to the cold source, while in a conventional reactor, only a small fraction of neutrons are dedicated to the source. The smaller size of the reactor will make it a practical research tool, economically available to an average research university. The reactor shall further be designed so as to produce a very high flux of cold neutrons; namely higher than the flux available at a reactor three orders of magnitude greater in power.

This innovative, optimistic proposal requires some explanation. Conventional (i.e., currently available) reactor sources are large, multi-purpose reactors that have one or more beam ports for cold neutron production/research. The manner in which they (the reactors)

produce the cold neutrons is simple and straightforward, but it is extremely inefficient. The thermal neutron population of the reactor follows the well known Maxwell-Boltzmann distribution. A certain fraction of these neutrons are at energies far lower than the energy of the spectral temperature of the neutron distribution. All neutrons of greater energy are then filtered out and further moderated to make up the cold neutron beam.

Because of the natures of the two processes, neutron production by spallation is often considered superior to neutron production by fission (as in a reactor). Fission, the splitting of a heavy nucleus by an externally introduced neutron of energy less than approximately 10 MeV, results in the production of one to three neutrons, depending on the fissionable isotope, its temperature, and the neutron energy. For example, an average of 2.042 neutrons is emmitted per neutron absorbed (capture or fission) in ^{235}U at 600 C, in a thermal neutron flux. This corresponds to a gain of approximately one neutron per fission event. However, fission also deposits considerable energy in the fuel, some 200 MeV per fission in the above case.

Spallation, on the other hand, is the breaking off of nucleons from the nucleus by highly energetic particles. There is no clearly defined threshold for spallation reactions. When the energy of the incident particle is on the order of 100 MeV or greater, the reaction is commonly accepted to be spallation. Spallation reactions produce a large number of neutrons. The spallation of ^{238}U by 1 GeV protons produces 40 neutrons per event. Such a spallation also deposits some

2000 MeV of energy into the target. Simple arithmetic will show that a fission reaction generates far more energy per neutron than does a spallation reaction, by a factor of four in the above illustration.

This comparison, however, presupposes that the reactor flux which one considers is the flux in the fuel region. This is indeed the case in the design process of nearly all nuclear reactors. However, when one realizes that the goal of a neutron source is to maximize the available neutrons while minimizing the power, one sees that this design process is not optimum, if one is designing a neutron source rather than a power reactor.

This brings us to the flux trap concept, developed by Ergen.[1] Ergen's concept considers a reactor with a moderator-filled cavity (the flux trap) at the center of a shell of fissionable material. Fission neutrons from the shell are thermalized in the cavity, leading to a peaking of the flux in the cavity. The moderator would ideally have a small absorption cross section, and good thermalization properties. This suggests the use of heavy water as the moderator in the central cavity. Osredkar and Stephenson[2] suggest the use of a filter or selective absorber between the fuel shell and the moderator cavity. This filter would be transparent to the fast neutrons produced in the core, and black to thermal neutrons, suggesting perhaps light water as a material to use for the filter.

In this way, once a fast neutron is thermalized in the moderator region, it is not lost by diffusion back into the core, raising the reactor power. Were the filter white rather than black, neutrons in the center of the cavity would be conserved (a positive effect), but

neutrons thermalized in the fuel or the external reflector would be reflected back through the fuel shell, raising the power (a negative effect).

Our proposal is to create a low power reactor having the sole purpose of creating a peak cold neutron flux, at a location that can conveniently produce a neutron beam. As described above, we shall consider a basic configuration involving a central moderator region (probably heavy water), a selective filter (probably light water), and a shell core or fuel region. In addition, we will include a reflector of some sort outside the shell core so as to direct as many neutrons as possible back into the central region.

This basic configuration shall be used for preliminary calculations, in order to optimize various flux trap features. The operational parameter of greatest importance is the ratio of the peak thermal flux (presumably at the center of the flux trap) to the reactor power.

The next step in the design of our cold source is to further slow the neutrons in the flux trap to the desired temperature. This is accomplished by employing a very low temperature moderator, on the order of 20 K. The moderator could be made separate from the above-described moderator, by having the cold moderator be the very center of the cavity, with the warmer moderator in an annular shape forming the outside of the cavity. The filter, core, and reflector regions would be unaffected. The design might also be effective if the moderator region were entirely at the lower temperature. Using a moderator at only one temperature might, however, be impossible from

an engineering standpoint, as the heat deposition associated with the slowing-down of the neutrons might lead to exorbitant refrigeration requirements.

A difficulty arises here. In a conventional neutron source, the neutrons are produced and then "sent to" the cold moderator. In our reactor, the cold moderator is an integral part of the neutronic design of the system. This necessitates cross section data for possible cold moderator materials beyond what is currently needed or, in fact, available. An additional part of the design process then includes work to make available reliable, usable cross section data for cold moderator materials.

Finally, additional regions are required for maintenance of the cold moderator. This might include a layer of liquid helium for refrigeration, a layer of bismuth for gamma shielding, and a layer of thermal insulation.

The computer modeling of the reactor is done using diffusion theory for first approximations, and discrete ordinates for situations where diffusion is not sufficient, as well as for final calculations involving cold moderators.

Diffusion theory calculations are performed by the code DODMG.[3] Discrete ordinates calculations are performed by the code ANISN.[4]

II. NEUTRON SCATTERING FACILITIES

Neutron scattering facilities, especially in the United States, are rather limited. As a measure of this, one can observe the amount of "user-time" (time at a facility by researchers not connected with that facility) requested as compared to such time actually granted. At most facilities with user programs, such programs are not generally able to adequately meet the demands of the research community. This deficiency is largely due to restrictions which could be alleviated by an increase in the number and/or quality of available facilities, e.g., beam time, instrument scientist time, etc.

As an example of this shortage, at the Intense Pulsed Neutron Source, a division of Argonne National Laboratory, approximately 325 experiment-days were available, as compared to some 625 requested.[5] Similarly, at the Los Alamos Neutron Scattering Center (LANSCE), "beam time was over-subscribed by a factor of about two in 1988."[6]

Some major neutron scattering facilities available throughout the world are listed below, in Table I.

The greater number of facilities listed in the United States, as compared with those listed in Europe, should not be taken to mean that the United States has more such facilities, but rather that information concerning U.S. facilities is more readily available. In actuality, Europe has a much larger pool of neutron scattering facilities, available to both private concerns and the research community at large, than does the United States.[7]

Table I. Sampling of major neutron scattering facilities (s; spallation, r; reactor)

DESIGNATION	LOCATION	TYPE
HFIRII	Oak Ridge National Laboratory, USA	r
HFBR	Brookhaven National Laboratory, USA	r
HFR	Institut Laue-Langevin, France	r
IPNS	Argonne National Laboratory, USA	s
ISIS	Rutherford-Appleton Laboratory, UK	s
KENS	National Laboratory for High Energy Physics, Japan	s
LANSCE	Los Alamos National Laboratory, USA	s
MURR	University of Missouri (Columbia), USA	r
NISTR	National Institute of Standards and Technology, USA	r
SINQ	Paul Scherrer Institute, Switzerland	s

The capabilities of various neutron scattering facilities are quite diverse. For example, the Institut Laue-Langevin has 40 spectrometers, including specific hot, thermal, and cold neutron sources, associated with its 57 MW reactor.[7] At the other extreme of our above mentioned facilities, all of which are well respected, is, for example, the MURR at the University of Missouri (Columbia). MURR is a 10 MW reactor with nine spectrometer units.[7] Even lower in capability are many university research reactors (URRs) not listed above.

The generally excepted criterion for a "good" scattering facility is a high neutron flux. Such a flux is necessary for accurate, efficient, and timely research. It is generally accepted that a thermal flux of at least 10^{13} neutrons/cm^2-sec is required for state-of-the-art problems.[7] This implies a reactor power (if indeed the facility is reactor-based), of at least 2 MW, when the reactor is designed according to conventional considerations. A list of some

state-of-the-art reactor facilities, and their available thermal fluxes, is given in Table II.

Table II. Peak thermal flux available at some reactor-based neutron scattering facilities[8]

FACILITY	POWER MW	THERMAL FLUX (10^{15} n/cm^2-sec)
HFIRII	200	4.0
HFBR	60	1.0
HFR	57	1.2
NISTR	20	0.2

As discussed in the previous chapter, spallation sources provide a greater neutron flux, compared to the thermal power produced in the core or target, than do reactor sources (if one is looking at the flux in the core region of the reactor). A list of the "peak" thermal fluxes available at some spallation sources appears in Table III. One should note that the performance of a spallation source is not really measured in this manner, but we use the "peak" thermal flux as a means of comparison.[8] This comparison is suitable only in the most general comparisons. A pulsed, spallation source requires several parameters to accurately characterize it, including pulse shape, width, frequency, etc.

Table III. Peak thermal fluxes available at some spallation-based neutron facilities

FACILITY	PEAK THERMAL FLUX (10^{15} n/cm^2-sec)
IPNS	0.4
ISIS	10.0
LANSCE	15.0

In spite of the above arguments, a high thermal neutron flux is not the sole criterion for a truly world-class neutron scattering facility. Spectrometer units, data acquisition and analysis systems, and support scientists are also required for a state-of-the-art facility. However, vital research can be and is carried out at smaller facilities.[9,10] The Institut Laue-Langevin in Grenoble, France has developed a program of cooperation with a network of smaller, university based facilities throughout Europe. The environment at a university based facility is far more conducive to original, developmental work than is the environment at a large user facility. There are several reasons for this phenomenon. At large facilities with broad user programs, competition is stiff for limited beam and instrument time. Additionally, user's travel time often prohibits long term development of experiments at such facilities. Thus, many new techniques are developed at small facilities and then imported to the larger facilities. Furthermore, many improvements are made in instrumentation at one facility and exported to the rest. Additionally, many experiments would not require a truly state-off-the-art neutron source for any but the final portion of the project. Such a project could be initiated at a university based facility, and the final stage of the project, requiring more accuracy or more efficiency, could be completed at the larger facility.

For these reasons, a viable program of cooperation between major, state-of-the-art neutron scattering facilities and smaller, less advanced facilities can greatly benefit both classes of facilities.

Such a program would have tremendous impact on the state of neutron scattering in the United States. The flux trap reactor design, being a university scale reactor source, would greatly facilitate such an exchange program.

III. THE GRANADA MODEL FOR THE CALCULATION OF SCATTERING CROSS SECTIONS OF MOLECULES

A model for analytically determining integral cross section data, most notably those data required for reactor physics calculations, has been developed by Granada.[11] This model is fairly simple, and thus the synthetic scattering function that it produces, $T(Q,\omega,E_0)$, is not an accurate approximation to the true scattering function, $S(Q,\omega)$. This is not, however, the purpose of the model. The model does produce accurate approximations to integral cross sections, namely the total scattering cross section (σ_T), and the energy transfer kernels (σ_0 and σ_1). These quantities can then be used to calculate transport coefficients: the mean scattering cosine ($<\mu>$), the transport cross section (Σ_{tr}), the diffusion coefficient (D), etc.

A. The Hypotheses behind Granada's Model

Granada's model employs two main hypotheses: First, the scattering system is assumed to be an ideal molecular gas, meaning that the translational motion of the center of mass of any molecule is that of a free particle. This assumption is valid as long as the time scale involved in the collision is shorter than the time scale characteristic of the diffusive motion of the molecule. For ordinary reactor systems, this would imply neutron energies on the order of millielectron volts. This, at first, seems to present a difficulty, as we wish to use the model to evaluate cross sections for low energy neutrons. However, we are interested only in the cross sections of

cold moderators, at a temperature far lower than that in conventional systems. The lower temperature of the scattering molecules means that the time scale corresponding to the diffusive motion, and thus allowed for the collision, is much larger, permitting lower neutron energies.

The second hypothesis assumes that the rotational and vibrational degrees of freedom are not coupled. This approximation to the real situation is valid only when the amplitude of atomic oscillations (with respect to their equilibrium positions in the molecule) is small when compared to the interatomic distances in the molecule. This assumption will also be enhanced at low molecular temperature. Furthermore, this assumption will not be inhibited by lower neutron energy.

We may therefore assume that the assumptions leading to the creation of Granada's model are reasonably applicable at lower molecular temperatures. As the accuracy of the model has been shown to be good at higher temperatures, we shall therefore have little reason to question it at lower temperatures, even when the neutron energies we consider are lower than those intended in the model's original purpose.

B. The Synthetic Scattering Function, $T(Q,\omega,E_0)$

The foundation of Granada's model, as with any other model, is the scattering function, $S(Q,\omega)$. This is used to obtain the double differential cross section,

$$\frac{d^2\sigma}{d\Omega\, dE} = \frac{k}{k_0}\frac{1}{4\pi}\sum_{\nu}\sigma_{\nu}\, N_{\nu}\, S_{\nu}(Q,\omega), \qquad (1)$$

where k and k_0 are the modulus of the scattered and incident wave vectors, respectively, ν indexes the species of nuclide in the molecule, each species with N_ν atoms present, each having a bound scattering cross section of σ_ν, and $S_\nu(Q,\omega)$ is the self part of the scattering function (of the ν-th constituent atom).

The double differential cross section can be manipulated in various ways to yield nearly any quantity of interest in reactor physics calculations. If one uses the true scattering function, this is analytically possible only in the simplest of situations. Granada, however, introduces a synthetic scattering function, $T_\nu(Q,\omega,E_0)$[11] To be used in place of $S_\nu(Q,\omega)$ in Equation (1). This $T_\nu(Q,\omega,E_0)$ is simple enough to perform the appropriate mathematical manipulations analytically. [For a development of this function, see the Appendix, where a portion of Granada's work[12] appears.] This equation can be integrated to give the desired cross section information.

Most other parameters of interest (i.e., $\langle\mu\rangle$, Σ_{tr}, etc.) can be obtained from the energy transfer kernels, σ_0 and σ_1. These kernels are defined as the zero-th and first order coefficients of a Legendre polynomial expansion of the double differential cross section.

C. Results of the Model

The accuracy of the model is demonstrated in Granada's work,[13] and is shown (albeit less extensively) here. Hereafter, any results referred to as "the results of the model" shall be from this work, and results quoted from Granada (or elsewhere) will be explicitly pointed out. Results are given for the total cross section and the σ_0 and σ_1 energy transfer kernels, for light water only.

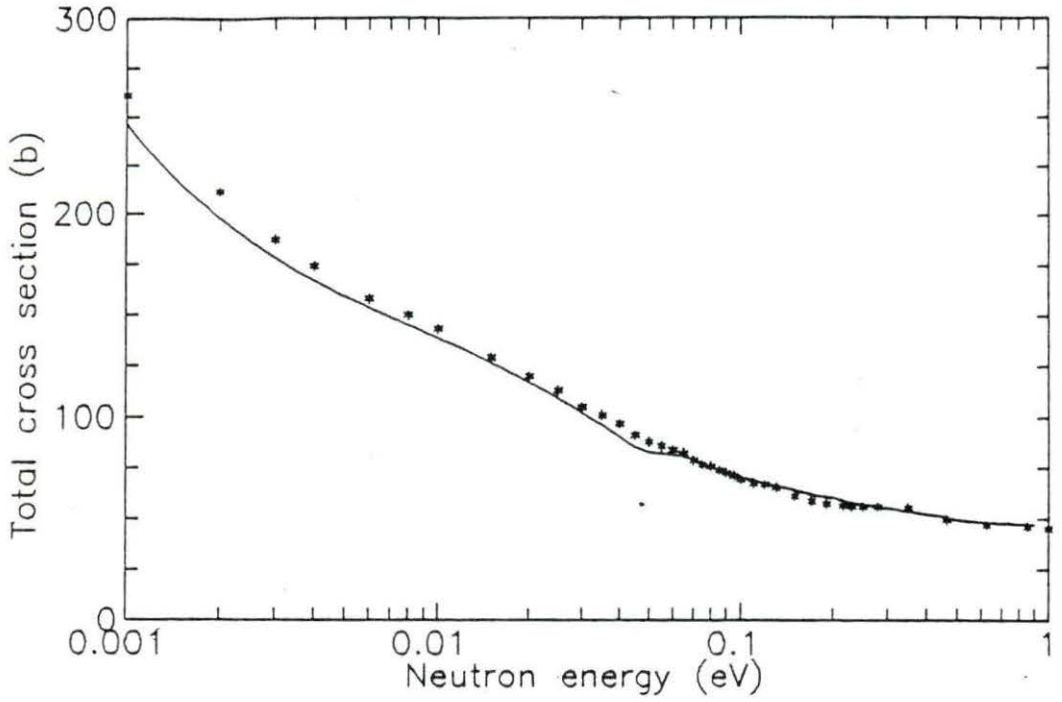

Figure 1. Comparison of synthetic model predictions to tabulated values for light water at 293 K (solid line is model, points are from code DODMG[3])

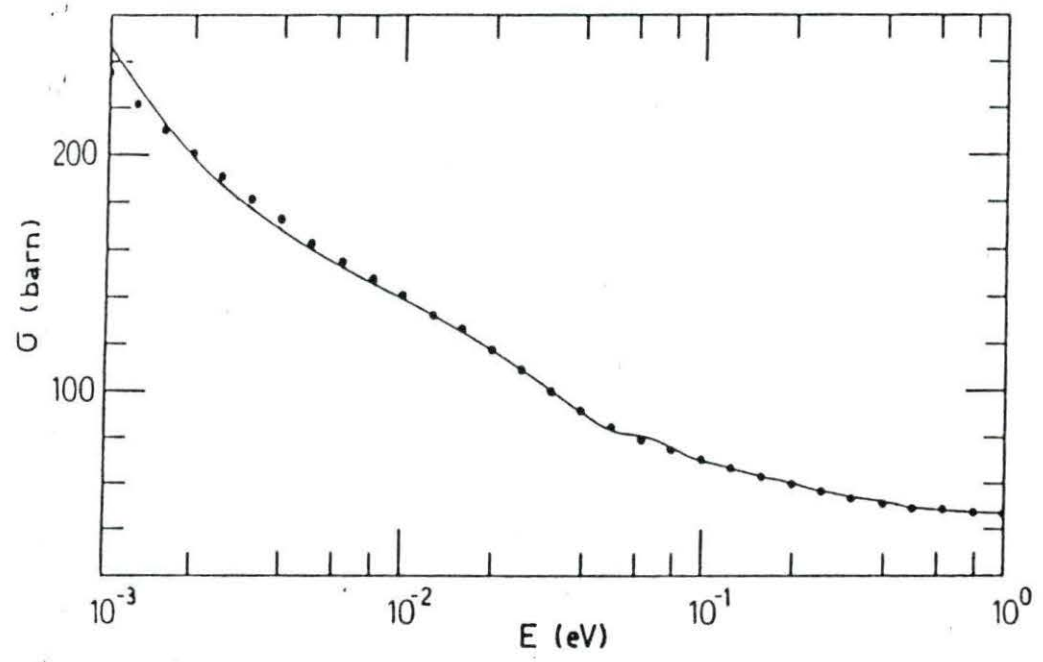

Figure 2. Comparison of Granada's model's predictions to tabulated values for light water (from Granada[11])

The model requires, as input, information about the dynamic structure of the molecule. The data used in these calculations are the same used in Granada's calculations,[13] appearing in the Appendix.

Figure 1 shows the total cross section of water over a range of energy of interest in typical reactor calculations. The figure also shows, for purposes of comparison, tabulated data taken from DODMG. Both the calculated and the tabulated data are for light water at 293K. One should notice small "humps" in both sets of data. These humps occur at neutron energies close to the energies of the various internal modes of the molecule. Figure 2 is a similar figure, taken from Granada, which compares calculations obtained from Granada's model with experimental data from Russell et al., cited in Granada.

Figure 3 shows the isotropic scattering kernel for water. The isotropic kernel is defined as the coefficient of the zero-th term in a Legendre polynomial expansion of the double-differential cross section, expressed by

$$\sigma_0(E_0,E) = 2\pi \int_{-1}^{1} \frac{d^2\sigma}{d\Omega\, dE}\, d(\cos\theta). \qquad (2)$$

The figure shows the kernel for three broadly spaced incident neutron energies in the thermal energy region. The peaks in the data correspond to the incident neutron energies. The "hump" on the upscattering side for the lowest incident energy is due to the annihilation of rotational phonons. This feature does not appear at higher incident energies because the contribution is smeared out by larger recoil energies. Figure 4, taken from Granada, contains similar data, and compares it to calculations using GASKET-FLANGE.

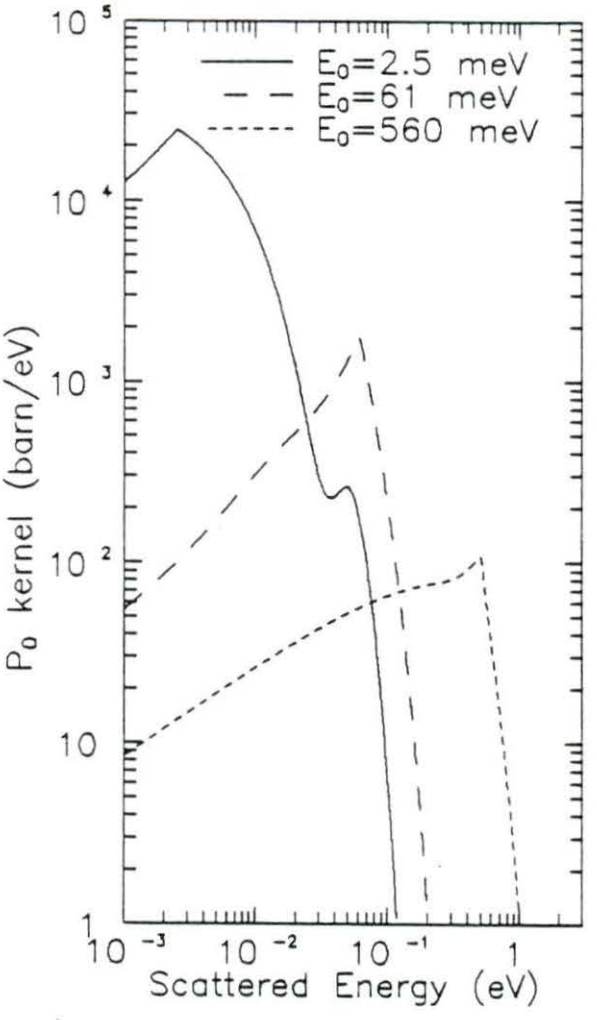

Figure 3. The P_0 energy transfer kernel of light water at 293 K

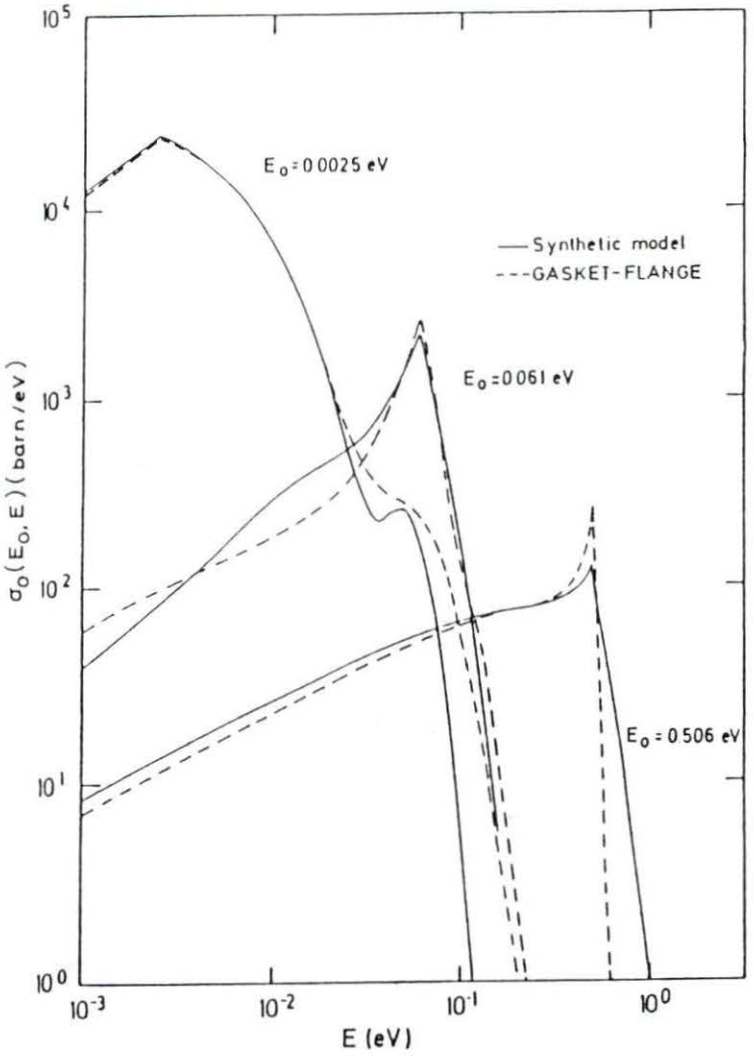

Figure 4. Comparison of Granada's model's predictions of P_0 energy transfer kernel for light water at 293 K with GASKET-FLANGE calculations (from Granada et al.)

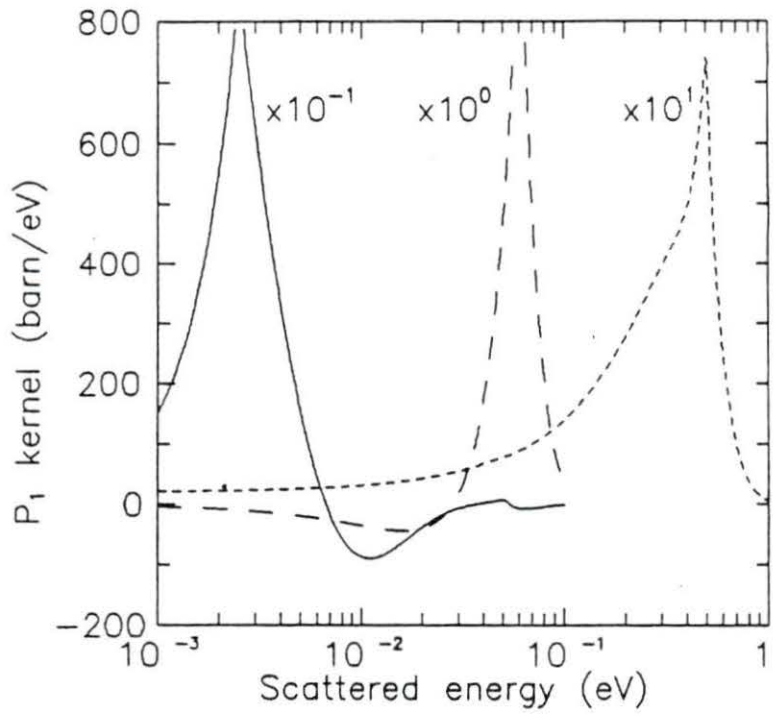

Figure 5. The P_1 energy transfer kernel of light water at 293 K (note different scale factors for each curve, other notation as in Figure 3)

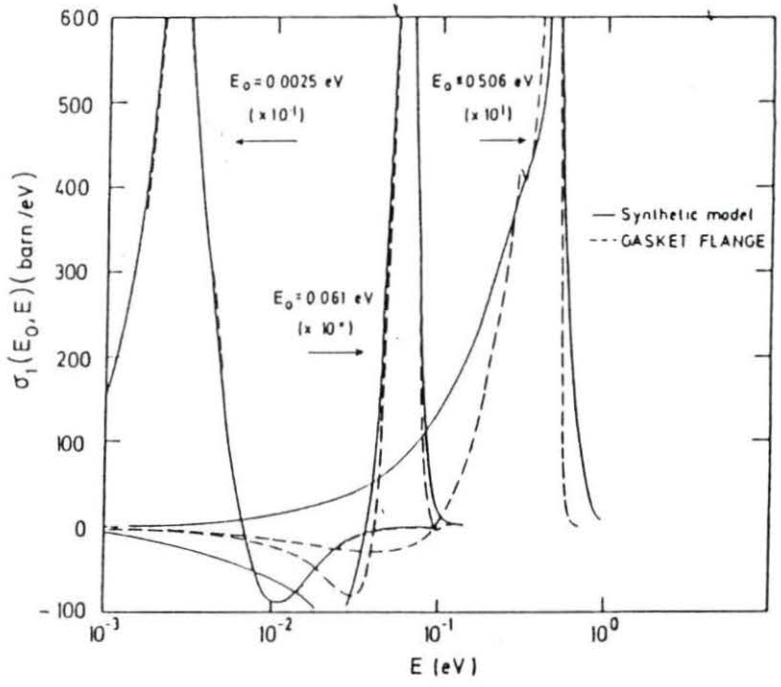

Figure 6. Comparison of Granada's model's predictions for the P_1 energy transfer kernel with GASKETT-FLANGE calculations for light water at 293 K, from Granada et al. (note different scale for each incident energy)

Figure 5 shows the first anisotropic scattering kernel, defined as the first order coefficient of the expansion of the double differential scattering cross section in Legendre polynomials. This kernel is given by

$$\sigma_1(E_0,E) = 2\pi \int_{-1}^{1} \frac{d^2\sigma}{d\Omega\, dE} \cos\theta\, d(\cos\theta). \qquad (3)$$

Figure 6, taken from Granada et al.,[13] shows the first anisotropic kernel as predicted by Granada's model, and compares it to GASKET-FLANGE calculations. Please note that the scale in both Figures 5 and 6 is shifted for the separate incident neutron energies, and that the boundaries of the two figures are different.

These figures demonstrate the accuracy of Granada's model, and further demonstrate the correctness of the current model. Unfortunately, cross section data at lower energies are unavailable for comparison, even though such data are what is truly desired of the model.

D. Conclusions about the Model

From the above results, including the results presented in Granada's work, the model can be assumed to be an accurate procedure for calculating parameters to use in reactor physics calculations. Specifically, we can assume that the model will produce accurate values for the various integral cross sections of low temperature molecules at low neutron energies.

IV. THE FLUX TRAP REACTOR

As mentioned earlier, the basic design of the reactor will includes a central moderator cavity, a selective filter, a core in a spherical annulus, and a reflector around the outside. Fuels examined for suitability and optimization are uranium dioxide, uranium metal, and a solution of uranyl nitrate ($UO_2(NO_3)_2$). The uranium concentration in the solution fuel, as well as the enrichment in each fuel are optimized as well. Moderators examined are heavy water and light water. The materials examined for use in the filter region are light water, heavy water, and beryllium. Finally, beryllium and beryllium oxide are considered for the reflector region.

A. The Optimization Procedure

The figure of merit for which the design is optimized is the ratio of the flux in the central, moderator region to the total power.

In order to optimize the design, each combination of the above materials is examined, considering different concentrations and/or enrichments of fuel to be different materials. The optimization procedure involves performing search calculations on the thickness of the fuel region for each separate configuration. In the search calculation, the thermal flux in the center of the moderator cavity is compared to the total power generated in the core, to obtain the "flux-to-power" ratio. The thickness of the filter region and the moderator are varied separately, for each different fuel material. The outer reflector was assumed to extend to infinity.

The calculations were performed with the computer codes DODMG[3] and ANISN-PC.[4] DODMG calculations were performed on an IBM XT compatible personal computer (with numeric coprocessor). The ANISN-PC calculations were performed on a COMPAQ 80386/80387 personal computer. Cross section data used were drawn from the DODMG libraries, with the exception of data from the Granada model. The code used for the Granada model appears (in diskette form) with this work. This code was also operated on a personal computer.

1. The fuel material

There is no great difference in the flux-to-power ratio observed for different forms of fuel. The metallic fuel shows slightly better characteristics than does either the solution or the oxide fuel, with respect to the flux-to-power ratio. This effect is presumably due to the reduction in core thickness possible with the higher density of ^{235}U atoms. The core thickness does reach a region of diminishing returns, however, once the thickness falls below approximately one centimeter. Other details are revealed, however, that make the choice of the appropriate fuel less clear; namely, the power distribution through the core region is extremely uneven. This uneven power distribution could cause great problems in solid fuels, both with burnup profiles and with temperature gradients. The burnup is extremely uneven in either case. The temperature gradient does not present as great difficulty to the metallic fuel as to the oxide fuel, but might still create unacceptable stresses. In addition, the solution fuel lends itself to the annular shape of the core as well as

it would to any other shape, while the metallic fuel might present machining difficulties. Finally, at the high concentration required (see below), the solution fuel might develop stability problems. It therefore appears that the best choice would be the metallic fuel, should it prove equal to the burnup and temperature distribution requirements.

2. Core concentration/enrichment

The effect on the flux-to-power ratio of varying the concentration of the fuel solution from one to nine molar appears to be similar to the effect of varying the fuel material. The greater the molarity, the thinner the core thickness required to achieve criticality. This effect is, however, subject to diminishing marginal returns once the solution rises above approximately seven molar. As the solution fuel is not selected as the optimum choice, it is not further considered.

The enrichment of the fuel is varied from three to ninety per cent (by weight). The inclusion of lower enrichment fuel is suggested by Osredkar and Stephenson.[2] The amount of ^{235}U should therefore be high enough to utilize those thermal neutrons returning from the reflector region and those not absorbed by the filter region. As suspected by Osredkar and Stephenson, a greater fast fission factor does lead to a greater flux-to-power ratio, but this effect is countered by the decrease in core thickness enabled by higher enrichment. This effect is very pronounced at low enrichment (less than ten per cent), but less so over a range of high enrichment

(twenty to ninety per cent). Since the intrinsic purpose of this project is an economical reactor, the trade-off between greater cost for very high enrichment and marginally greater neutron production does not seem to justify said expense.

3. Filter/moderator material

The nature (and magnitude) of the flux-to-power ratio is very strongly dependent upon the material composing the filter region. Figure 7 shows the flux-to-power ratio for three different materials. The figure shows the inferiority of a heavy water filter, and (somewhat less clearly) the insuitability of the beryllium filter. The data in this figure are for a filter one centimeter in thickness, and metal fuel with twenty per cent enrichment.

The effect of different materials in the moderator region is also quite distinct. Hydrogen absorption is very detrimental to the central flux when a light water moderator is used. Thus, for both the filter and the moderator regions, the appropriate materials to use are as suggested by Osredkar and Stephenson;[2] namely, light water for the filter, and heavy water for the moderator.

4. Filter thickness

Figure 8 shows the effect of different filter thicknesses on the flux-to-power ratio. The strong influence of the filter thickness can be put into the form of a question, "where does the greater absorption of the hydrogen counteract its greater slowing down capability?" The answer, apparent from Figure 8, is approximately three centimeters. This figure displays data for metallic fuel with twenty per cent enrichment.

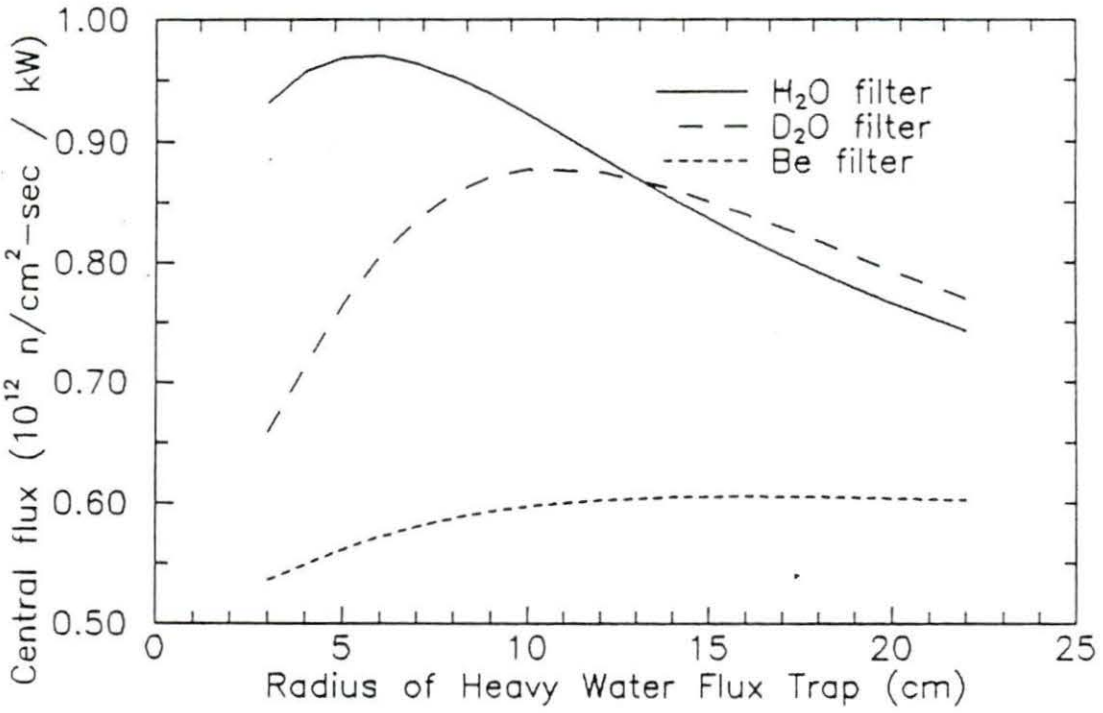

Figure 7. Comparison of flux-to-power ratio attainable with different filter materials

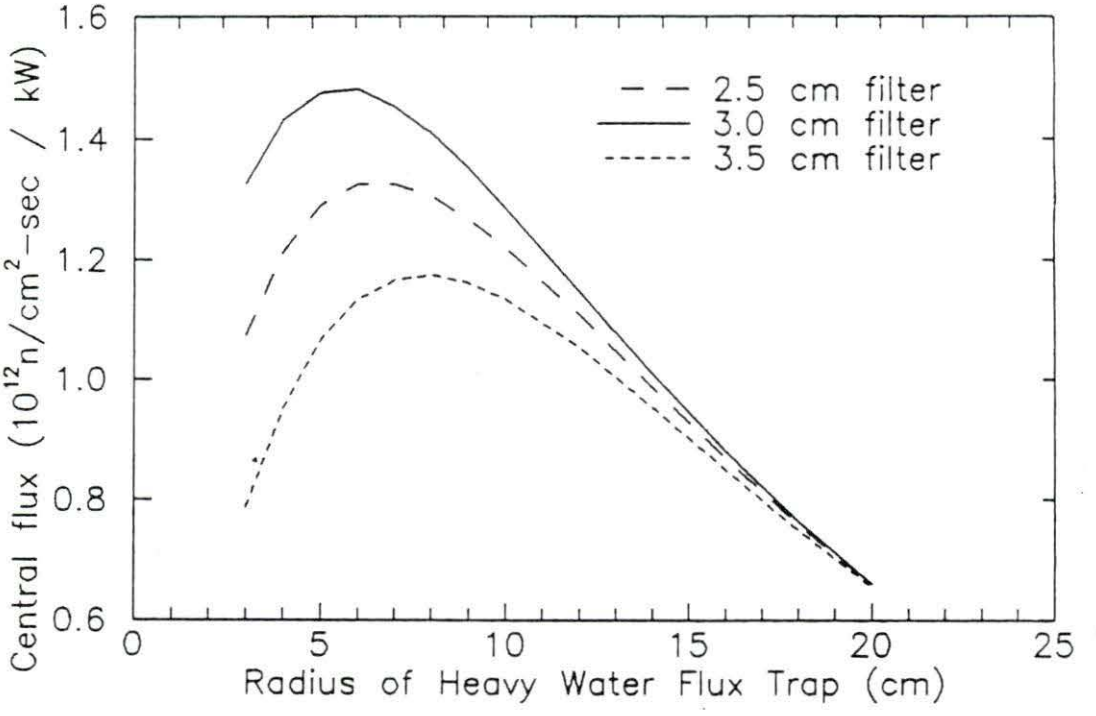

Figure 8. Comparison of flux-to-power ratios attainable with filters of different thicknesses

5. Moderator radius

As can be seen from Figures 7 and 8, the optimum moderator radius is between five and eight centimeters. Using larger moderators might prove necessary for engineering constraints, but such changes would involve considerable sacrifice in the flux-to-power ratio. The greatest ratio is found at a seven centimeter moderator radius, with a three centimeter filter.

6. Reflector material

The difference in reflector materials, between beryllium and beryllium oxide, is nearly undetectable. In fact, both situations are quite adequately dealt with in the calculations by considering albedo conditions on the outer boundary of the core. The difference in materials gives rise to differences in the albedos on the order of parts-per-ten thousand.

Based on the above data, we have determined the "optimum" flux trap configuration to consist of a seven centimeter heavy water moderator, a three centimeter light water filter, a metallic uranium fuel enriched to three weight per cent and either a beryllium or a beryllium oxide reflector.

B. The Inclusion of a Cold Moderator

The inclusion of a cold moderator--heavy water at 20K in the center of the moderator region--in the model has no discernible detrimental effects on the flux-to-power ratio. The mean neutron temperature in the center of such a region some six centimeters in

diameter is 26K. The inclusion of such a cold moderator is therefore deemed not to decrease the flux-to-power ratio in the reactor, or in fact, significantly alter the neutronic parameters of the reactor. The presence of the cold moderator would, however, bring about certain additional engineering considerations, mostly concerned with refrigeration.

C. Engineering Considerations for Cold Moderators

The most significant engineering consideration facing the design is the gamma heating of the cold moderator region, possibly beyond the capability of currently available refrigeration units. A simple, highly conservative gamma heating model for the above-mentioned configuration indicates that a cold moderator region with a radius of three centimeters (of seven total for the entire moderator) would receive approximately 2 W of gamma heating per kW of reactor power. Table IV indicates the estimates for gamma heating with the inclusion of a bismuth shield between the filter and the outer (warm) moderator region.

As indicated by Table IV, the inclusion of 2.0 cm of bismuth between the filter and the moderator would decrease this heating to 0.6 W/kW reactor power, while reducing the central flux by less than 20 %. The model is highly conservative, and more realistic models could reduce this considerably.

Table IV. Estimated gamma heating on moderator with bismuth shield, and associated effect on available flux (3 cm cold moderator, 4 cm warm moderator, 3 cm filter)

Bi shield thickness (cm)	γ heating per unit power W/kW	Neutron transmission (%)
0.0	2.069	100.0
0.1	1.934	99.0
0.2	1.808	98.1
0.3	1.695	97.1
0.4	1.589	96.2
0.5	1.492	95.2
0.6	1.402	94.3
0.7	1.319	93.4
0.8	1.241	92.5
0.9	1.169	91.6
1.0	1.102	90.7
1.1	1.040	89.8
1.2	0.982	88.9
1.3	0.928	88.0
1.4	0.877	87.2
1.5	0.829	86.3
1.6	0.785	85.5
1.7	0.743	84.6
1.8	0.704	83.8
1.9	0.667	83.0
2.0	0.632	82.2

D. Application of the Design

As indicated by Figures 7 and 8, the maximum flux-to-power ratio attainable for the different configurations considered is approximately 1.5×10^{12} n/cm^2-sec / kW reactor power. Referring to Table II, one can see that the use of a 100 kW reactor of the flux trap design could produce a thermal flux similar to the thermal flux from the NISTR reactor, which has a power 200 times higher. In addition, typically designed cold sources will suffer a penalty of three to four orders of magnitude between thermal flux and cold flux,

while this design will suffer a penalty of, at most, twenty per cent. The implications of this difference are striking. A 100 kW reactor is small enough that most major universities, as well as some private industries, could afford the purchase and upkeep costs, especially when one considers the dividends possible.

CHAPTER V. CONCLUSIONS

Neutron scattering is a valuable, necessary research tool. A national program of cooperation between small, university scale neutron scattering facilities and larger, state-of-the-art facilities would greatly advance the science in the United States. A reactor source is far more suitable to a small, university related facility than is a spallation source.

A. The Design

The optimum flux trap design configuration found in Chapter IV was found to be a set of concentric spherical shells of the following composition and dimensions (from the center outward): three centimeters of heavy water at ~20 K, two centimeters bismuth, four centimeters heavy water at room temperature, three centimeters of light water, approximately one centimeter of metallic uranium, enriched to twenty weight percent, and an essentially infinite beryllium or beryllium oxide reflector. This design was calculated to be able to produce a thermal flux, in the central moderator, of approximately 8×10^{13} n/cm^2-sec, with the reactor operating at some 100 kW. In addition, this thermal flux could be converted to a cold flux with unprecedented ease and efficiency, enabling a cold flux (spectral temperature of ~26 K) of some $1\text{~}5 \times 10^{13}$ n/cm^2-sec. Such a cold flux would likely require considerable refrigeration (~75 W at 20 K), but this trade-off should be acceptable, given the dividends.

B. Future Work

Recommendations for further work include an improved model for gamma heating/shielding, a thermal stress analysis of metallic fuel under a very uneven power profile, and an examination of the potential perterbations caused by the inclusion of a neutron guide tube to tap the central flux.

VI. APPENDIX

A. Input Data[13]

TABLE I. Values of the parameters for the synthetic model used in the calculations. Energies are given in eV and masses in neutron mass units.

Parameter \ Atom	H_2O		D_2O		C_6H_6	
	H	O	D	O	H	C
$\hbar\omega_1$	0.070		0.050		0.120	
$\hbar\sigma_1$	0.021		0.021		0.030	
M_1	2.380	342.0	4.390	190.5	1.531	17.67
$\hbar\omega_2$	0.205		0.150		0.380	
$\hbar\sigma_2$	0.018		0.018		0.018	
M_2	4.768	746.2	13.25	427.4	3.345	392.3
$\hbar\omega_3$	0.481		0.310			
$\hbar\sigma_3$	0.018		0.018			
M_3	3.180	373.1	6.817	203.7		

B. Excerpt Showing Equations

arguments and characteristic features will be given here.

The scattering system is considered to be an ideal molecular gas at temperature T, which means that the translational motion of the molecules' center of mass is taken as that corresponding to a free particle.

Although the motion of the molecular unit may be severely hindered in a real system due to the presence of its neighbors, it is only for very slow neutrons that this collisional regime will become dominant. Consequently, we consider a low-energy limit for the incident neutrons such that the experimental time scale is shorter than that characteristic of diffusive motion. The attainment of this condition clearly depends on the particular system under study, but for most real cases it implies neutron energies (a few meV) which are outside the region of main interest in reactor-physics calculations.

The internal degrees of freedom of the molecule are assumed to be not coupled. This is a first approximation to the real situation which is valid as long as the amplitudes of the atomic oscillations around their equilibrium positions are small compared to the interatomic distances in the molecule. Each of the λ internal modes is represented by an Einstein oscillator with angular frequency ω_λ and effective mass M_λ.

From the requirement that the free-atom cross section be approached at high neutron energies (large compared with $k_B T$ and the largest $\hbar\omega_\lambda$), a normalization condition for these masses is obtained:

$$\frac{1}{M_{\text{mol}}}+\sum_\lambda \frac{1}{M_\lambda}=\frac{1}{M}\ , \tag{1}$$

where M_{mol} is the molecular mass and M is the mass of the nucleus under consideration (in neutron mass units). An additional constraint is imposed on the rotational mass M_R, namely

$$\frac{1}{M_{\text{mol}}}+\frac{1}{M_R}=\frac{1}{\mathcal{M}}\ , \tag{2}$$

where $\mathcal{M}$ is the (spherically averaged) tensorial mass introduced by Sachs and Teller[15] to describe the combined effect of translations and rotations. The remaining vibrational masses are determined by the relative weights of the related amplitude vectors.

Correspondingly, at epithermal neutron energies the scattering nuclei are viewed as possessing a kinetic energy associated with a temperature $\overline{T}$ given by

$$k_B\overline{T}=k_B T+\sum_\lambda \frac{M}{M_\lambda}(E_\lambda-k_B T)\ , \tag{3}$$

where E_λ is the mean energy of the λ oscillator.

From the analysis of the forms that $S(Q,\omega)$ takes for small and large energy transfer $\hbar\omega$ in the scattering process, a function $T(Q,\omega;E_0)$ is proposed which uses the incident neutron energy E_0 as a variation parameter. The main characteristics of the molecular dynamics are then retained through the introduction of an effective mass, temperature, and vibrational factors. This is achieved by the use of the Krieger-Nelkin[16] procedure for orientational averages, and by the introduction of switching functions P_λ defined by

$$P_\lambda(E_0)=\frac{\exp\left[-\left|\frac{E_0-\hbar\omega_\lambda}{\hbar\sigma_\lambda}\right|^2\right]+\sqrt{\pi}\,\frac{\hbar\omega_\lambda}{\hbar\sigma_\lambda}\left[1+\operatorname{erf}\left|\frac{\hbar\omega_\lambda-E_0}{\hbar\sigma_\lambda}\right|\right]}{\exp\left[-\left|\frac{\hbar\omega_\lambda}{\hbar\sigma_\lambda}\right|^2\right]+\sqrt{\pi}\,\frac{\hbar\omega_\lambda}{\hbar\sigma_\lambda}\left[1+\operatorname{erf}\left|\frac{\hbar\omega_\lambda}{\hbar\sigma_\lambda}\right|\right]}\ , \tag{4}$$

where the quantities σ_λ are representatives of the width of the frequency spectrum in the vicinity of ω_λ.

Every P_λ tends to zero as the corresponding mode λ becomes fully excited from the point of view of the collision process, that is when a quasiclassical treatment is applicable. At the other end, the value of P_λ is 1 if the neutron cannot excite any of the λ-oscillator energy levels. At intermediate energies, the variation of P_λ should depend on the shape of that part of the molecular frequency spectrum associated with the mode λ. The expression given by Eq. (4) meets the above requirements and its supporting arguments are discussed in Ref. 13; its dependence on the temperature of the system is dictated by the shifting and broadening of the corresponding part of the frequency spectrum.[17]

An effective mass for the nucleus under consideration is defined by

$$\frac{1}{\mu}=\frac{1}{M_{\text{mol}}}+\sum_\lambda \frac{(1-P_\lambda)}{M_\lambda}=\frac{1}{M}-\sum_\lambda \frac{P_\lambda}{M_\lambda}\ . \tag{5}$$

In this way, μ takes values ranging from M_{mol} to M, according to the state of excitation of the different internal modes.

By requiring consistency between the first and second moments of the scattering function, an expression for the effective temperature τ is obtained:

$$\frac{k_B\tau}{\mu}=\frac{k_B T}{M_{\text{mol}}}+\sum_\lambda \frac{(1-P_\lambda)}{M_\lambda}E_\lambda=\frac{k_B\overline{T}}{M}-\sum_\lambda \frac{P_\lambda}{M_\lambda}E_\lambda\ , \tag{6}$$

where $k_B\overline{T}$ is given by Eq. (3). Clearly τ tends to T, the actual system temperature, or $\overline{T}$, the "free-atom temperature," according to whether all P_λ are 1 or zero, respectively.

Finally, an effective Debye-Waller factor Γ is defined by

$$\Gamma=\sum_\lambda \frac{P_\lambda}{M_\lambda}\frac{(2n_\lambda+1)}{\hbar\omega_\lambda}\ , \tag{7}$$

...ere n_λ is the thermally averaged occupation number ...the λ mode.

With the above definitions, the atomic synthetic ...ttering function which describes a scattering process ...h energy and momentum exchange $\hbar\omega$ and $\hbar Q$, re...tively, is written as

$$...(Q,\omega;E_0)=S_{\mu,\tau}(Q,\omega)\exp\left[-\Gamma\frac{\hbar^2Q^2}{2}\right]+C_{\mu,\tau}(Q,\omega)\ . \tag{8}$$

$$...(Q,\omega)=\tfrac{1}{2}\sum_\lambda p_\lambda\left[n_\lambda\hbar^2Q_+^2S_{\mu,\tau}(Q_+,\omega_+)\exp\left[-\Gamma\frac{\hbar^2Q_+^2}{2}\right]+(1+n_\lambda)\hbar^2Q_-^2S_{\mu,\tau}(Q_-,\omega_-)\exp\left[-\Gamma\frac{\hbar^2Q_-^2}{2}\right]\right], \tag{10}$$

...h $p_\lambda\equiv P_\lambda/(M_\lambda\hbar\omega_\lambda)$.

Here, $Q_\pm$ is the modulus of the scattering vector cor...ponding to a fictitious incident energy $E_{0,\lambda}^{\pm}=E_0\pm\hbar\omega_\lambda$. This correction term accounts for one-...non processes which may be operative for those ...s of thermal- or collision-induced excitations but ...h a neutron energy not high enough to allow a ...nclassical treatment of the corresponding mode.

With the notation

$$S_{\mu,\tau}^{KN}(Q,\omega)=S_{\mu,\tau}(Q,\omega)\exp\left[-\Gamma\frac{\hbar^2Q^2}{2}\right], \tag{11}$$

...finally obtains

$$...(Q,\omega;E_0)=S_{\mu,\tau}^{KN}(Q,\omega)-\sum_\lambda p_\lambda\left[n_\lambda\frac{\partial}{\partial\Gamma}S_{\mu,\tau}^{KN}(Q_+,\omega_+)+(1+n_\lambda)\frac{\partial}{\partial\Gamma}S_{\mu,\tau}^{KN}(Q_-,\omega_-)\right]. \tag{12}$$

This is the mathematical expression of the synthetic ...del. It does not pretend to be a real scattering func...a model for molecules, insofar as the full dynamics of ...atomic motion is not accounted for in a detailed ...ner and also because only the incoherent contribu...n to the scattering process is considered. In Sec. III, ...ever, we take advantage of its formal simplicity to ...ve analytical expressions for some magnitudes of in...st in reactor physics.

...ork is in progress involving applications of the syn...ic model to other fields, examples of which are the ...ation of inelasticity corrections in neutron ...ction work on molecular liquids[18] and the optimiza...n of neutron production and time response of modera...used in pulsed neutron sources.[19]

III. EVALUATION OF CROSS SECTIONS

The most basic magnitude which is experimentally ac...ble is the double-differential cross section. For the ...ering of an unpolarized beam of neutrons from a ...ular system, it is given by

$$\frac{d^2\sigma}{d\Omega\,dE}=\frac{k}{k_0}\sum_\nu\frac{\sigma_\nu}{4\pi}N_\nu T_\nu(Q,\omega;E_0)\ , \tag{13}$$

where k_0 and k denote the (modulus of) incident and scattered neutron wave vectors, respectively, ν runs over the species of nuclide in the same environment, each with a number N_ν of them and with a bound scattering cross section σ_ν.

This magnitude has been[20] and continues to be[17,21] a valuable source of information on the dynamics of condensed systems. However, from the point of view of neutron thermalization studies, the measurement of double-differential cross sections was mainly aimed at the determination of a continuous frequency spectrum according to the Egelstaff extrapolation method.[2] This quantity or its Fourier transform, the (self-) velocity-velocity correlation function, is related to the width function in the frame of the Gaussian approximation,[22] so that its knowledge permits us to obtain the scattering law by numerical Fourier transformation of the intermediate scattering function.[7] Although well supported on physical grounds, this is usually a rather lengthy and expensive procedure and furthermore, the information thus acquired is unnecessarily rich for most reactor-physics problems.

A. Energy-transfer cross sections

Following in line, the next quantities of interest are the energy-transfer kernels, defined as the coefficients of the double-differential cross section expansion in a base of Legendre polynomials.

1. The P_0 kernel

We start by considering the isotropic scattering kernel, which is

$$\sigma_0(E_0,E)=2\pi\int_{-1}^{1}d(\cos\theta)\frac{d^2\sigma}{d\Omega\,dE}\ , \tag{14}$$

or, in terms of the synthetic model

$$\sigma_0(E_0,E)=\frac{1}{4\pi}\sum_\nu\sigma_\nu N_\nu\sigma_0^\nu(E_0,E)\ , \tag{15}$$

where

$$\sigma_0^{\nu}(E_0,E)=2\pi\frac{k}{k_0}\int_{-1}^{1}d(\cos\theta)T_{\nu}(Q,\omega;E_0)\ . \tag{16}$$

This is the contribution to the molecular scattering kernel corresponding to each atomic species ν. In what follows we will drop this index when writing expressions for the atomic contributions, keeping in mind that eventually they must be added according to Eq. (15) to give the molecular cross section.

To proceed with the calculation, it is useful to remember that $S^{KN}_{\mu,\tau}(Q,\omega)$ as defined in Eq. (11) can also be written

$$S^{KN}_{\mu,\tau}(Q,\omega)=\exp\left[-\frac{(1-f)\hbar\omega}{2k_B\tau'}\right]S_{\mu',\tau'}(Q,\omega)\ , \tag{17}$$

with

$$f=(1+4\Gamma k_B\tau\mu)^{-1/2},\quad \mu'=f\mu,\quad \tau'=f\tau\ ,$$

and $S_{\mu',\tau'}(Q,\omega)$ denoting a free-gas scattering function, Eq. (9), but for particles of mass μ' at temperature τ'.

Then, from Eq. (16) and the principal term of Eq. (12), we have

$$2\pi\frac{k}{k_0}\int_{-1}^{1}d(\cos\theta)S^{KN}_{\mu,\tau}(Q,\omega)$$

$$=\exp\left[-\left[\frac{1-f}{2}\right](x_0^2-x^2)\right]\sigma_{\mu',\tau'}(E_0,E)$$

$$\equiv\sigma_0^0(E_0,E)\ , \tag{18}$$

where we are using the notation

$$\sigma_{\mu',\tau'}(E_0,E)=2\pi\frac{k}{k_0}\int_{-1}^{1}d(\cos\theta)S_{\mu',\tau'}(Q,\omega) \tag{19}$$

and $x_\alpha^2=E_\alpha/k_B\tau'$.

Similarly, we obtain

$$2\pi\frac{k}{k_0}\int_{-1}^{1}d(\cos\theta)S^{KN}_{\mu,\tau}(Q_\pm,\omega_\pm)=\left[1\pm\frac{x_\lambda^2}{x_0^2}\right]^{1/2}\exp\left[-\left[\frac{1-f}{2}\right](x_0^2-x^2\pm x_\lambda^2)\right]\sigma_{\mu',\tau'}(E^{\pm}_{0,\lambda},E) \tag{20}$$

for the contributions originated in the correction term of the synthetic function. Collecting the previous results, we formally can write the (isotropic) atomic scattering kernel as

$$\sigma_0(E_0,E)=\sigma_0^0(E_0,E)-\sum_\lambda p_\lambda\left[n_\lambda\left[1+\frac{x_\lambda^2}{x_0^2}\right]^{1/2}\frac{\partial}{\partial\Gamma}\sigma_0^0(E^{+}_{0,\lambda},E)+(1+n_\lambda)\left[1-\frac{x_\lambda^2}{x_0^2}\right]^{1/2}\frac{\partial}{\partial\Gamma}\sigma_0^0(E^{-}_{0,\lambda},E)\right]\ . \tag{21}$$

Clearly, it is the formal simplicity of the synthetic model that allows us to make further progress in this derivation, because in spite of the appearance of derivatives with respect to Γ in the last formula, we know the analytic expression[23] for the free-gas scattering kernel, Eq. (19). With the notation

$$\eta=\frac{\mu'+1}{2\mu'^{1/2}},\quad \rho=\frac{\mu'-1}{2\mu'^{1/2}}\ , \tag{22}$$

and after some lengthy algebra, we finally obtain

$$\sigma_0(E_0,E)=\exp\left[-\left[\frac{1-f}{2}\right](x_0^2-x^2)\right]\sigma_{\mu',\tau'}(E_0,E)$$

$$+2\mu' k_B\tau'\sum p_\lambda\left[n_\lambda\left[1+\frac{x_\lambda^2}{x_0^2}\right]^{1/2}\chi(E^{+}_{0,\lambda},E)+(1+n_\lambda)\left[1-\frac{x_\lambda^2}{x_0^2}\right]^{1/2}\chi(E^{-}_{0,\lambda},E)\right]\ . \tag{23}$$

Here we have defined

$$\chi(E_0,E)=\exp\left[-\left[\frac{1-f}{2}\right](x_0^2-x^2)\right]\left[\left[1+\frac{x_0^2-x^2}{2}\right]\sigma_{\mu',\tau'}(E_0,E)+\xi_{\mu',\tau'}(E_0,E)\right]\ , \tag{24}$$

with

$$\sigma_{\mu',\tau'}(E_0,E)=\frac{\pi\mu'}{2k_B\tau' x_0^2}\{\operatorname{erf}(\eta x-\rho x_0)\mp\operatorname{erf}(\eta x+\rho x_0)-\exp(x_0^2-x^2)[\operatorname{erf}(\rho x-\eta x_0)\mp\operatorname{erf}(\rho x+\eta x_0)]\}\ , \tag{25}$$

and

$$\xi_{\mu',\tau'}(E_0,E)=\frac{\pi\mu'}{2k_B\tau' x_0^2}[(x_0^2-x^2)\exp(x_0^2-x^2)[\operatorname{erf}(\rho x-\eta x_0)\mp\operatorname{erf}(\rho x+\eta x_0)]$$

$$-\frac{1}{(\pi\mu')^{1/2}}((x+x_0)\exp[-(\eta x-\rho x_0)^2]\mp(x-x_0)\exp[-(\eta x+\rho x_0)^2]$$

$$+\exp(x_0^2-x^2)[(x+x_0)\exp[-(\rho x-\eta x_0)^2]\mp(x-x_0)\exp[-(\rho x+\eta x_0)^2]])\ , \tag{26}$$

where the upper (lower) sign holds for upscattering (downscattering) processes.

The formulas given above, Eqs. (23)–(26) with the definitions (22), are the analytic expression of the isotropic energy-transfer kernel derived from the synthetic scattering function. It is convenient to make a few comments on some of its features.

As the model itself, the kernel contains a principal and a correction term as clearly displayed in Eq. (23), the correction part involving the evaluation of quantities at the fictitious neutron energies $E^{\pm}_{0,\lambda}$. The term proportional to n_λ accounts for phonon annihilation processes, while that containing the factor $(1+n_\lambda)$ corresponds to phonon creation. Of course, this latter term only exists when the incident neutron energy is high enough to allow the transfer of a quantum of energy to the λ oscillator.

The assumption that an Einstein oscillator represents the relevant part of the actual frequency spectrum could be unrealistic, specially for rotations where usually a fairly broad band of eigenfrequencies shows up. In the spirit of our prescription,[13] this is accounted for through the widths σ_λ associated with each eigenfrequency ω_λ, such that the phonon contributions $\chi^{\pm}_\lambda$ are evaluated at the effective frequencies $\omega^*_\lambda=\omega_\lambda-\sigma_\lambda$.

2. The P_1 kernel

The first anisotropic scattering kernel is defined by

$$\sigma_1(E_0,E)=2\pi\int_{-1}^{1}d(\cos\theta)\cos\theta\frac{d^2\sigma}{d\Omega\,dE}\ ,$$

and, according to the synthetic model, it will be represented by an expression of the form

$$\sigma_1(E_0,E)=\sigma_1^0(E_0,E)+2\mu' k_B\tau'\sum_\lambda p_\lambda\left[n_\lambda\left[1+\frac{x_\lambda^2}{x_0^2}\right]^{1/2}\kappa(E^+_{0,\lambda},E)+(1+n_\lambda)\left[1-\frac{x_\lambda^2}{x_0^2}\right]^{1/2}\kappa(E^-_{0,\lambda},E)\right], \tag{27}$$

where the functions σ_1^0 and κ arise from the principal and correction terms, respectively. Their explicit forms are derived in the Appendix, with the result

$$\sigma_1^0(E_0,E)=\frac{(xx_0)^{-1}}{2}[(x_0^2+x^2)\sigma_0^0(E_0,E)-2\mu'\chi(E_0,E)]\ , \tag{28}$$

and

$$\kappa(E_0,E)=\frac{(x_0x)^{-1}}{2}\left\{\left[(x_0^2+x^2)\left[1+\frac{x_0^2-x^2}{2}\right]-\frac{\mu'}{2}[12+6(x_0^2-x^2)+(x_0^2-x^2)^2]\right]\sigma_0^0(E_0,E)\right.$$
$$\left.+\exp\left[-\left[\frac{1-f}{2}\right](x_0^2-x^2)\right]\left[[x_0^2+x^2-2\mu'(4+x_0^2-x^2)]\xi(E_0,E)-2\mu' f\frac{\partial}{\partial f}\xi(E_0,E)\right]\right\}, \tag{29}$$

where the functions χ and $\xi_{\mu',\tau'}$ are given by Eqs. (24) and (26), respectively, while σ_0^0 denotes the principal term of the isotropic kernel, Eq. (23).

It is worthwhile to emphasize that $\sigma_0^0(E_0,E)$ and $\sigma_1^0(E_0,E)$ are the analytical expressions of the P_0 and P_1 energy-transfer kernels, respectively, corresponding to a nucleus bound to a semirigid molecule. By this we mean a situation in which its complete dynamics can be described in terms of an effective translational motion modulated by a vibrational factor [cf., Eq. (11)], as first proposed by Krieger and Nelkin.[16] Furthermore, by taking the limit $\Gamma\to 0$ in those formulas one regains the P_0 and P_1 kernels corresponding to a monatomic gas of particles of mass μ in equilibrium at temperature τ.

B. Total cross section

The expression of the total cross section derived from the synthetic model has been already presented,[13] but for the sake of completeness we write down the formulas again using the notation of the preceding sections.

The total cross section per molecule for an incident neutron energy E_0 is

$$\sigma^T(E_0)=\sum_\nu\frac{\sigma_\nu}{4\pi}N_\nu\sigma_\nu^T(E_0), \tag{30}$$

where ν, σ_ν, and N_ν have the same meaning as in Eq. (13) and $\sigma_\nu^T(E_0)$ denotes the atomic contribution.

For this quantity we obtain

$$\sigma_\nu^T(E_0)=\sigma^{KN}(E_0)+\frac{1}{\Gamma}\sum_\lambda p_\lambda\left[n_\lambda\left[1+\frac{x_\lambda^2}{x_0^2}\right]^{1/2}\Lambda(E^+_{0,\lambda})+(1+n_\lambda)\left[1-\frac{x_\lambda^2}{x_0^2}\right]^{1/2}\Lambda(E^-_{0,\lambda})\right], \tag{31}$$

where the first term of the right-hand side is the result derived by Krieger and Nelkin[16] for the total cross section corresponding to the scattering function $S^{KN}_{\mu,\tau}(Q,\omega)$ as defined in Eq. (11):

$$\sigma^{KN}(E_0)=\frac{\pi\mu'}{Z\Gamma k_B\tau'}\{\mathrm{erf}(Z^{1/2})-(1-C)^{1/2}\,\mathrm{erf}[Z^{1/2}(1-C)^{1/2}]\exp(-ZC)\}\ . \tag{32}$$

The other quantities appearing in Eq. (31) are

$$\Lambda(E_0)=\frac{\pi\mu'}{Zk_B\tau'}\left[\frac{1}{\Gamma}\mathrm{erf}(Z^{1/2})-A\left[\frac{Z}{\pi}\right]^{1/2}e^{-Z}-(1-C)^{1/2}e^{-ZC}\mathrm{erf}[Z^{1/2}(1-C)^{1/2}]\left[\frac{1}{\Gamma}+AZ+\frac{A}{2(1-C)}\right]\right], \quad (33)$$

with

$$Z=\mu' x_0^2 ,$$

$$C=\frac{1-f^2}{[1+\mu'(\mu'+2f)]} ,$$

and

$$A=4\mu' k_B\tau'\left[\frac{1-C}{f+\mu'}\right]^2 .$$

Of course, the value of σ^T thus obtained coincides at each incident neutron energy E_0 with the integral over final energies of the synthetic scattering kernel, Eq. (23).

By an analogous reason to that already discussed in Sec. III A 1, the functions $\Lambda(E^{\pm}_{0,\lambda})$ are evaluated at effective phonon frequencies $\omega^*_\lambda=\omega_\lambda-\sigma_\lambda(x^{*2}_\lambda=\hbar\omega^*_\lambda/k_B\tau')$. The term involving $\Lambda(E^{-}_{0,\lambda})$ in Eq. (31) accounts for the contribution due to phonon creation processes and only exists when $E_0\geq\hbar\omega^*_\lambda$.

We must emphasize again that the phononlike contributions to the cross sections are originated in the correction terms introduced to account for those scattering processes involving small energy transfers. On the other hand, the principal (or λ independent) term collects the inelastic contributions as the neutron energy increases, because all the terms in the phonon expansion are then accounted for through the short collision-time treatment of the molecule internal degrees of freedom.

The forms adopted by the total cross section, Eq. (31), in the limits of low- and high-incident neutron energy (compared with the characteristic excitation energies $\hbar\omega_\lambda$) are easily obtained from the prescribed variation (Sec. II) of the effective quantities μ, τ, and Γ.

For $E_0\to 0$ we find from Eqs. (4) to (7):

$$\mu\to M_{\mathrm{mol}},\quad \tau\to T,\quad \text{and}\quad \Gamma\to\Gamma_{\max}=\sum_\lambda\frac{(2n_\lambda+1)}{M_\lambda\hbar\omega_\lambda} . \quad (34)$$

Also, from Eq. (32)

$$\sigma^{KN}(E_0\to 0)\simeq\alpha\left[\frac{k_BT}{\pi M_{\mathrm{mol}}E_0}\right]^{1/2} , \quad (35)$$

where

$$\alpha=8\pi M^2_{\mathrm{mol}}/[(1+M_{\mathrm{mol}})^2+4\Gamma_{\max}M_{\mathrm{mol}}k_BT] .$$

There is no possibility of phonon creation in this limit of subthermal incident neutrons, and then we finally obtain

$$\sigma^T_v(E_0\to 0)\simeq E_0^{-1/2}\left[\alpha\left[\frac{k_BT}{\pi M_{\mathrm{mol}}}\right]^{1/2}+\frac{(k_BT)^{1/2}}{\Gamma}\sum_\lambda p_\lambda(x_0^2+x_\lambda^2)^{1/2}\Lambda(E^{+}_{0,\lambda})\right] , \quad (36)$$

where the variables entering in the definition of Λ, Eq. (33), are evaluated according to the values of the basic parameters as given in (34). It is clear that in the case of a hypothetical nonvibrating molecule ($\Gamma=0$), the above expressions reduce to the well-known result[4] for a gas of particles of mass M_{mol} at temperature T.

In the opposite limit, when $E_0\gg\hbar\omega_\lambda$ for all λ, we find that $\mu\to M$, $\Gamma\to 0$, and

$$\tau\to\bar{T}=T+\sum_\lambda\frac{M}{M_\lambda}\left[(n_\lambda+\tfrac{1}{2})\frac{\hbar\omega_\lambda}{k_B}-T\right] ,$$

because all P_λ's are then equal to zero. The synthetic model reduces to the form $S_{M,\bar{T}}(Q,\omega)$ and therefore the total cross section in this energy range is given by[4]

$$\sigma^T_v(E_0\gg\hbar\omega_0)\simeq\frac{4\pi M^2}{(1+M)^2}\left[\left[1+\frac{1}{2y}\right]\mathrm{erf}(y^{1/2})+\frac{1}{\sqrt{\pi y}}e^{-y}\right] , \quad (37)$$

with $y=ME_0/k_B\bar{T}$. Moreover, in the limit of very high neutron energy one recovers the asymptotic expression[24]

$$\sigma^T_v(E_0\to\infty)\simeq\frac{4\pi M^2}{(1+M)^2}\left[1+\frac{1}{2}\frac{k_B\bar{T}}{ME_0}\right] , \quad (38)$$

which clearly shows that in this energy limit the atoms are seen as possessing a kinetic energy associated to the temperature $\bar{T}$ rather than T. This is a general result valid for any state of the scattering system.[25]

C. Diffusion parameters

With the magnitudes previously defined in this section, we are in a position to evaluate a number of quantities of interest in neutron- and reactor-physics calculations. These are the transport coefficients whose expressions can be found in standard textbooks,[23] but we write them here for the sake of completeness as they are used extensively in the following paper to test our model predictions.

The average cosine of the scattering angle is given by

$$\langle\cos\theta(E_0)\rangle=\int_0^\infty dE\,\sigma_1(E_0,E)\Big/\int_0^\infty dE\,\sigma_0(E_0,E) , \quad (39)$$

where σ_0 and σ_1 are the zero- and first-order angular moments of the double-differential cross section, respectively, which are expressed by Eqs. (23) and (27) according to the synthetic model.

For a molecular system, the macroscopic transport cross section is

$$\Sigma_{\mathrm{tr}}(E_0)=N_m\sigma^T(E_0)[1-\langle\cos\theta(E_0)\rangle] , \quad (40)$$

where N_m denotes the molecular number density, $\sigma^T(E_0)$ is the total cross section per molecule as defined

VII. REFERENCES

[1]W. K. Ergen, Proceedings of the Second United Nations International Conference on the Peaceful Uses of Atomic Energy, United Nations Publication (United Nations, Geneva, 1958), Vol. 10, p. 181.

[2]M. Osredkar and R. Stephenson, Proceedings of the Second United Nations International Conference on the Peaceful Uses of Atomic Energy, United Nations Publication (United Nations, Geneva, 1958), Vol. 10, p. 174.

[3]Alfred F. Rohach, computer code DODMG (Iowa State University Department of Mechanical Engineering, Ames, Iowa, 1990).

[4]D. Kent Parsons, computer code ANISN-PC (EG&G Ortec, Idaho Falls, Idaho, 1987).

[5]B. S. Browsn, in Proceedings of the 10th Meeting of the International Collaboration on Advanced Neutron Sources (ICANS X), Institute of Physics Conference Series No. 97, edited by D. K. Hyer (IOP Publishing Ltd., Bristol, 1989), p. 44.

[6]R. Pynn, in Proceedings of the 10th Meeting of the International Collaboration on Advanced Neutron Sources (ICANS X), Institute of Physics Conference Series No. 97, edited by D. K. Hyer (IOP Publishing Ltd., Bristol, 1989), p. 50.

[7]Committee on University Research Reactors, University Research Reactors in the United States-their Role and Values (National Academy Press, Washington, D.C., 1988), p. 108.

[8]J. M. Carpenter and W. B. Yelon, in Methods of Experimental Physics, edited by D. L. Price and K. Sköld Academic Press, Inc., (Harcourt Brace Jovanovich, New York, NY), 23 A, p. 120.

[9]R. Pynn and B. E. F. Fender, "Neutron Scattering in Europe," Phys. Today 38 (1), 49 (1985).

[10]Committee on University Research Reactors, University Research Reactors in the United States-their Role and Values (National Academy Press, Washington, D.C., 1988), p. 109.

[11]J. R. Granada, Phys. Rev. B 31, 4167, 1985.

[12]J. R. Granada, Phys. Rev. A 36, 5585, 1988.

[13]J. R. Granada, V. H. Gillette, and R. E. Mayer, Phys. Rev. A 36, 5594, 1988.

VIII. ACKNOWLEDGEMENTS

I would like express my warmest regards and thanks to Dr. Bernard Spinrad, my major professor, my mentor, and my friend. His creativity and insight inspired me repeatedly, and his encouragement was of incalculable assistance. I would also like to thank Dr. John Carpenter for sharing his enthusiasum for research with me, and Dr. Donald Roberts for teaching me to look at issues from other viewpoints.

I would like to extend my appreciation to Arnie Olson of Argonne National Laboratory for assistance with ANISN.

I would like to thank to my fiancé Angela, for her support and assistance in the completion of this work, and for her patience in dealing with my idiosyncracies.

Portions of this work were funded by the Department of Energy, through the Student Research Participation Program, and through a DOE Nuclear Engineering Fellowship.